Case Studies in Construction Materials 17 (2022) e01273

Contents lists available at ScienceDirect

Case Studies in Construction Materials

journal homepage: www.elsevier.com/locate/cscm

Case study

Fracture mechanics modeling of reinforced concrete joints strengthened by CFRP sheets

Farzad Hejazi [a], Hogr Karim [b], Hamid Kazemi [c], Shahriar Shahbazpanahi [d], Amir Mosavi [e,f,g,*]

[a] Department of Civil Engineering, University Putra Malaysia, Malaysia
[b] Civil Engineering Department, University of Halabja, Halabja, Kurdistan Region, Iraq
[c] Department of Civil Engineering, Faculty of Engineering, University of Minho, Portugal
[d] Department of Civil Engineering, Sanandaj Branch, Islamic Azad University, Sanandaj, Islamic Republic of Iran
[e] Faculty of Civil Engineering, Technische Universität Dresden, 01069 Dresden, Germany
[f] Institute of Information Engineering, Automation and Mathematics, Slovak University of Technology in Bratislava, Bratislava, Slovakia
[g] John von Neumann Faculty of Informatics, Obuda University, 1034 Budapest, Hungary

ARTICLE INFO

Keywords:
Connection
Concrete
Crack propagation
Fracture mechanics modeling
CFRP

ABSTRACT

Nowadays, fracture mechanics modeling for strengthening structural members is a challenging issue for structural engineers. The developed fracture mechanics modeling was applicable for identifying propagation of a crack in concrete structural members such as beam-column connections. In the present paper, a numerical model derived from nonlinear fracture mechanics is developed to simulate the propagation of a crack in Carbon Fiber Reinforced Polymers (CFRP)-strengthened the connection. To validate the proposed model, two beam-column connections were made and tested. By using the proposed model, the outputs of the CFRP-strengthened connections show good agreement with the experimental results (8–12 %). It was also observed that propagation of the crack in the beam was prevented by the CFRP sheets. The average decrease was 36.9 % of the crack length compared with the control connection. The findings revealed that cracks formed in the connection area in the control specimen while extensive cracks appeared in the beam in the specimen strengthened by CFRP sheets.

1. Introduction

One of the weak structural elements in concrete structures is the reinforced concrete (RC) connection [1–3]. Predictions of cracks in the RC beam-column connection are necessary [4,5]. Cracks in the connection create where the column and the beam intersect due to tension stress increases [6,7]. Thus, one of the best theories to predict the crack in the RC connection is the fracture mechanics theory [8–10]. Connections, which prepare for structure continuity, are a vital and important part of concrete structure [11–13] For that reason, the research on crack patterns is important [14,15]. Due to the complex behavior of the connections [16], an accurate crack fracture mechanics simulation for connections is essential. The fracture process zone (FPZ) and the strain energy release rate relation have become the fundamental concepts of nonlinear fracture mechanics of concrete structures. A crack can occur in the column connection (shear crack) or beam [17]. Cracks in the connection can fail the whole structure. Therefore, cracks in the connection are

* Corresponding author at: Faculty of Civil Engineering, Technische Universität Dresden, 01069 Dresden, Germany.
E-mail address: amir.mosavi@kvk.uni-obuda.hu (A. Mosavi).

https://doi.org/10.1016/j.cscm.2022.e01273
Received 30 April 2022; Received in revised form 14 June 2022; Accepted 26 June 2022
Available online 30 June 2022

more important than other forms of cracks. These types of cracks have been observed in some studies [18]. If a crack occurs in a connection, the beam reduces its load capacity. This situation should be avoided for concrete structures. To solve this issue, the crack needs to be shifted to an adjacent beam. Many researchers [19–23] have undertaken studies in the shear strength as well as behavior for different connection types. The examples include the study exterior and interior connections. The design of existing beam-column connections based on pre-1970s codes does not usually have adequate strength. The dissipation of the energy is therefore inadequate and hinging mechanisms are unsuitable resulting in extreme displacement and a fast decrease in strength. The current failures of whole structures clearly show that beam-column connections can initiate and result in the collapse of the structure [24]. Recently, many experimental studies have been carried out on beam-column connections to study their exact behavior under various parameters such as the amount and details of the reinforcemen [25,26] grade of concrete [27], the effect of longitudinal reinforcemen [28] shear reinforcemen [29–31] and effect of rebar diameter [32]. These only conducted experimental tests without any numerical validation. The results of these studies included the identification of joint shear, beam hinges and concrete confinement which are certainly important design factors as recommended by most codes [9,33].

On the other hand, connections can be retrofitted with Carbon Fiber Reinforced Polymers (CFRP) sheets [34–36]. Many studies have been carried out on CFRP-strengthened connections through experimental tests and many types of finite element models and analytical methods [37–39]. Experimental studies were done by Parvin et al. [40] on the strength of the connections using CFRP sheets under gravity load without any shear reinforcement at the core of the connection to enhance the performance of the connections. Ludovico et al. [41]studied the behavior of connections with various configurations of CFRP laminates. Akgüzel and Pampanin [42,43] studied the response of non-seismically designed connections strengthened by GFRP. Alhaddad et al. [44] deliberated a comparison in the effect of connections before and after upgrading it with CFRP and mortar. Xiaobing et al. [45] have also studied square CFRP-strengthened connections using experimental procedures. Singh et al. [46] steered static loading test on nine CFRP-strengthened RC beam-column connections, where two L-shape layers of CFRP were used for the connection. Experimental tests were conducted on eight connection subassemblies by Realfonzo et al. [47] Seven of the aforesaid connections were reinforced by using various CFRP methods and the remaining one was used as a target. Experimental tests were also carried out by Del et al. [33] on six connections with special CFRP-strengthened configurations. Bsisu and Hiari [48] presented theoretical research of a strengthening technique by CFRP using FEA aimed at improving the behavior of connections of their performance and the structures load-displacement. The effect of CFRP strengthening on RC connections was modeled by Baji et al. [49]. In this study, cracks were modeled by smeared crack elements. These studies indicated that strengthening with CFRP composites has moved the joint shear failure to the beam-column connection interface. Also, the shear strength connections have been improved by CFRP sheets; but, failures of beam were remarked in only a few samples, and in others, before a beam plastic hinge formed, CFRP debonded from the surface of the concrete.

However, in the above-mentioned studies, the propagation of crack based on nonlinear fracture mechanics in the tested connections has not been carried out. Thus, an accurate numerical simulation to assess the behavior of the connections strengthened by CFRP sheets is still under debate. The crack propagation has an important role on the capacity and fracture resistant of beam-column connection. Therefore, crack propagation modeling is also very important in connections and shows the significance of this research. Also, strengthening by CFRP sheets would be necessitated to prevent the crack propagation. Consequently, the goal of this study is to develop a more accurate prediction of crack propagation in RC connections strengthened with CFRP sheets. To achieve the abovementioned aim, a new numerical model for the prediction of the propagation of a crack in connections reinforced with CFRP under static load was developed and the new proposed model was validated by experimental tests on RC connections with and without CFRP strengthening.

2. Materials and methods

2.1. Proposed numerical model

In this section, a numerical simulation was introduced to model the propagation of the crack in RC connections strengthened with CFRP sheets. The crack propagation model for RC connection strengthened with CFRP sheet consists of four components: propagation of the crack modeling in control RC connections, modeling of soffit strengthened members, the slip modeling between CFRP and concrete, and modeling of side face strengthened connections. These components are briefly explained in the following sections. In order to analyze the crack propagation, 2D plane stress models by FEAPpv® program code were used [50]. In this program, the solution algorithm was written by the user subroutines (USER 1–4).

2.1.1. Crack modeling in control RC connections

In this study, only a flexural crack in the control connection was considered to simplify the analysis. A four-node, thin-layer interface element in USER 1 of FEAPpv Fortran programming was used [50] to model the fracture process zone. Choosing such an element enables us to consider the width of the FPZ in modeling. To estimate crack propagation in a connection zone, a crack is assumed to propagate when the tensile stress in the tip of the crack reaches connection shear stress [51]. Based on the experimental study by Goto and Jo [51] the relationship between the connection shear stress and concrete compressive strength was proposed. They stated that the shear stress of the connection zone is equal to $5\sqrt{f_c'}$ (f_c' is the concrete compressive strength). Thus, if the tensile stress in the crack tip reaches $5\sqrt{f_c'}$, value, a crack is propagated in the connection. Furthermore, they found that if the connection stress at the beam rebars is $4\sqrt{f_c'}$ value, connection shear failure will not occur. In addition, the crack will propagate in the beam if the tensile stress

in the crack tip is between $5\sqrt{f_c'}$ and $4\sqrt{f_c'}$.

Moreover, the concrete compression strut zone transfers shear stress (see Fig. 1). Thus, it is important to model the zone of the strut. The results presented by experimental data of Mitra and lowes [52] was used to model the strut zone and is expressed as follows:

$$\sigma_{cn} = f_{c_{strut}} \frac{w_{strut}\ cos\alpha_{strut}}{w} \tag{1}$$

where σ_{cn} is normal stress and f_{c_strut} is strut stress. The w_{strut} is the strut width and α_{strut} is the strut angle of inclination at the horizontal line. The w is the connection, width respectively (Fig. 1).

The strain energy release rates in this zone. According to [53], can be described as follows.

$$G_{cn} = \frac{\sigma_{cn}(x_1\text{-}x_2)}{2LB}, \tag{2}$$

To predict other cracks propagation in the beam or the column, the crack was assumed to propagate when the principal stress gets the concrete tensile strength. In the present model, the crack direction was simulated by a technique that a crack occurs along existing interface element boundaries [54].

2.1.2. Modeling of flexural-strengthened elements

Modeling flexural-strengthened concrete beams or connections can be carried out by attaching a layer of truss elements. The strengthening might be at the bottom and/or top of the member. The truss element is used to model the CFRP sheets by using an elastic material. The effects of flexural of CFRP strengthened connections on crack propagation criterion in concrete are vital. Thus, a numerical model based on nonlinear fracture mechanics should be developed. Let us consider a part of CFRP reinforced RC beam-column connection (See Fig. 2). The CFRP will increase the energy dissipation rate of connection. The amount of energy dissipated in the system can be determined by calculating the change in the potential energy of the system. This study obtained the energy dissipation rate of flexural-strengthened members by CFRP according to [55], can be described as follows:

$$R = \frac{E_F \delta^2}{2 b_f L'}, \tag{3}$$

where b_f, E_F, and δ are the width, the elastic modulus of CFRP, and the opening displacements of crack, respectively (Fig. 2). The L' is the mesh size. The USER 2 was the name of the subroutine that was used to simulate flexural-strengthened elements.

Eq. (3) was used to predict the CFRP effect as the crack propagates in concrete. Eq. (3) illustrates that if the length of the FPZ grows, the opening of the crack will be small. Therefore, the effect of the CFRP on preventing crack propagation is relatively small. As the length of the FPZ extends at a constant value, the role of the CFRP in resisting crack propagation increases. To date, no model has presented a convincing equation to predict the CFRP effect on crack propagation. Given that the CFRP is not located at the crack tip, the rate of energy dissipation due to the moment of couple caused by the CFRP force was ignored.

2.1.3. Modeling of side face strengthened elements

To simulate concrete substrate and side face reinforced by CFRP sheets, a composite model is needed. A finite element model was developed to simulate side face strengthened by CFRP sheets on the concrete elements (USER 3). To model crack propagation, a truss element was set at the tip of crack. A bar element with linear elastic was utilized to calculate the rate of strain energy dissipation by the CFRP. The rate of strain energy dissipation was calculated directly by using a virtual crack closure technique (VCCT) [55]. To compute the stiffness matrix for the interface element, the stress equilibrium on an element (Fig. 3) was expressed by:

$$\sigma = \sigma_{cn} + \rho_{FRP} \quad . \quad \sigma_{FRP}, \tag{4}$$

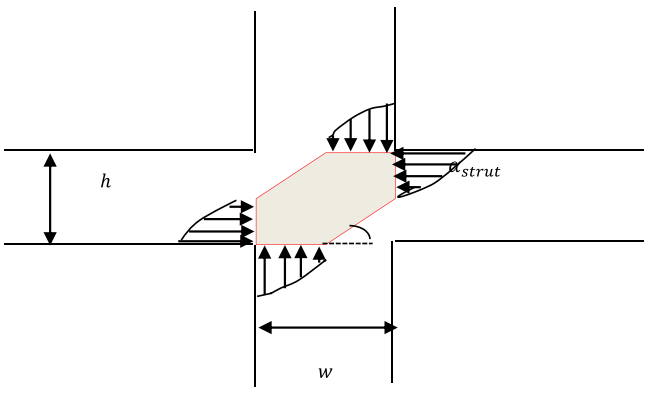

Fig. 1. Strut model in the RC beam-column connection zone.

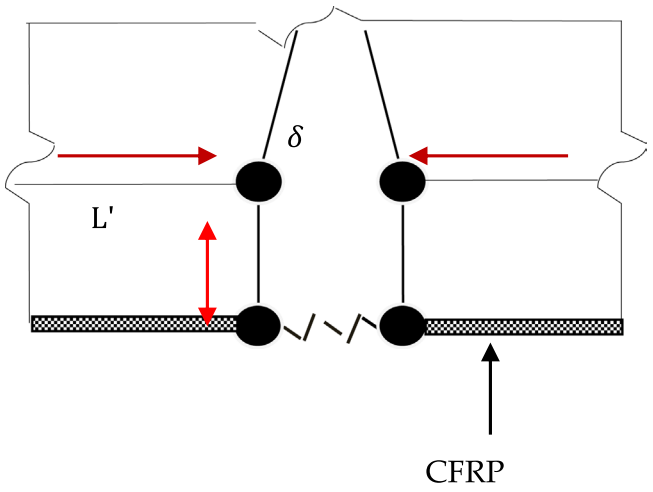

Fig. 2. Modeling of flexural strengthened joint by CFRP.

where σ is normal stress in the this zone of connection. The ρ_{FRP} is CFRP reinforcement ratios in the global x-directions. σ_{FRP} is stresses in the reinforcement composite. A small part of connection zone was shown in Fig. 4. As the interface, a bar element was set connecting nodes "1" and "2".

The strain energy release rates based on [56] were equal to:

$$G = \frac{\sigma\ (x_1\text{-}x_2)}{2L'B}, \tag{5}$$

where x_1 is displacement of node "1"and x_2 is corresponding value "2" in x direction. If $G + R > G_C$, the interface element was removed, the crack was propagated, and the stiffness of the interface element becomes zero. The G_C is the concrete critical fracture energy.

2.1.4. bond-slip model between CFRP and concrete

Correct modeling is essential to estimate the bond slip of CFRP sheets. In this research to consider interfacial shear stresses distribution between CFRP and concrete, the finite element model developed by Shahbazpanahi and Kamgar [57] was used to model the slipping in the CFRP-concrete interface in USER 4. An interface element was utilized. In the nodes, interface element cohesive forces were expressed by finite element methods. When the principal stress equals the maximum shear stress in the concrete and the CFRP interfaces, de-bonding happens. The CFRP behavior was elastic behavior but elastic–perfect plastic behavior was used to model the steel bars. Moreover, isoparametric elements with four-node are used for bulk concrete with isotropic behavior. Bar elements are used to model the longitudinal, stirrup steel, and soffit CFRP.

2.2. test setup of experimental samples

To validate the proposed model, a comprehensive experimental test on connection samples was conducted.

2.2.1. Specimens

The experiment consisted of two cross beam-column connections under static monotonic loading. One of the samples, (J-0), was the control connection (with no CFRP). The remaining sample, (J-1), was reinforced with CFRP sheets. The samples were designed following the ACI 318-63 code. The connections were supported in place by the bottom hinges. A support frame was used to fix the position. The columns were 400 mm × 400 mm cross-section dimensions and high of 2700 mm. The lengths of the beams were

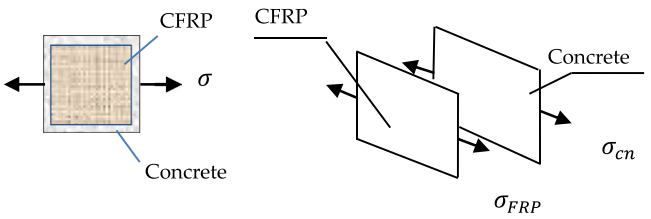

Fig. 3. Stresses in the concrete and the side face- CFRP.

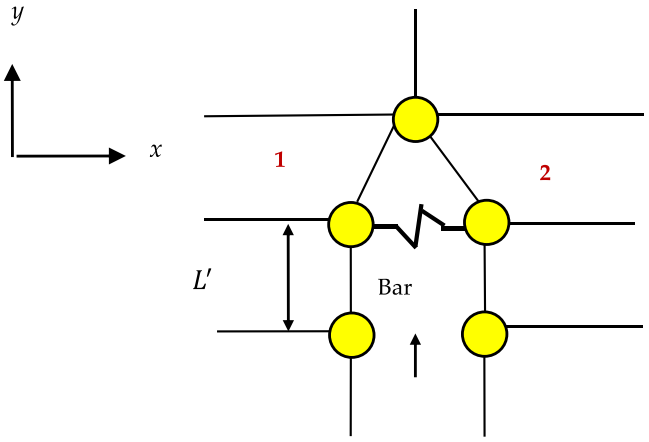

Fig. 4. An element of a concrete in connection zone.

1800 mm from the column face with a 300 mm × 300 mm cross-section. The eight steel bars (25 mm in diameter) were used in the columns. In the columns, transverse shear bars with 10 mm diameter were provided. According to ASTM D39 [58], Table 1 displays a mixed design to use in the connection.

The stirrups of column were used at 170 mm inside the connection and at 600 mm below and above the connection. The beams have two top longitudinal bars with 25 mm diameter. Moreover, the beams were reinforced by two bottom longitudinal bars with 20 mm diameter. The beam stirrup bars were a rectangular tie measuring 8 mm in diameter beginning at 50 mm from the column face. The transverse reinforcements of the beam measure rectangular stirrups measuring 8 mm in diameter starting at 50 mm from the face of the column. Details of the positions of the strain gauges of the control connection are shown in Fig. 5. The steel bars and transverse reinforcements have 400 MPa yield strengths. The concrete compressive strength was 21.5 MPa based on the test result of a standard cylinder. The steel reinforcement and CFRP sheets properties were listed in Table 2.

Fig. 6 illustrations the CFRP details the connection for sample (J-1). The connection was reinforced by 7 layers of CFRP laminates with thickness of 1.17 mm. Plastic hinges will form at the ends of the beams near the column. Thus, connection is strengthened by confining CFRP strengthening at potential plastic hinge locations. The CFRP sheets were applied in an L-shaped arrangement on the bottom and top surfaces of concrete. The length of these CFRP sheets for the connection was kept constant at 600 mm. Then, CFRP sheets were used around the beam for 150 mm to the right and left of the connection core. The widths of the CFRP wraps were 150 mm. Sheets were used round the column at 150 mm below and above the connection core.

2.2.2. Instrumentation

Instrument readings including strain gauges, load cells, and Linear Variable Differential Transformer (LVDT) were set to zero. The instruments were utilized to observe (1) load cells to measure column axial load, (2) strains in all beam and column bars via strain gauges, (3) four LVDTs to evaluate displacement at different locations, and (4) loads applied to the beams tips via two load cells on the specimen as shown in Fig. 7. Two LVDTs evaluated the displacements of beams tip and another two were used to measure the motion of the rigid connection. Strains in the concrete and steel bars at various locations were also obtained by electrical resistance strain gauges. The strain gauges locations on the transverse and longitudinal steel bars in the column and beam were presented in Fig. 7.

2.2.3. Set-up of the test

The test setup details for control connection (J-0) and the connection strengthened by CFRP (J-1) are shown in Figs. 8 and 9 respectively. The connection sample was loaded in the invariable axial force to the column. In the next stage, two the same forces were loaded to the tips of beams to model the gravity load effect. To measure the applied load, two load cells were used at the tips of beams. Moreover, the bottom of the column was supported by hinge support [Fig. 10]. Also, a roller support was specified at the top of the column and built with a 20 mm vertical slot.

The experimental was performed below a gradually rising monotonic load till the failure of the beam was achieved. Axial load at the top of the column using a static actuator was a constant load (150 kN). However, the applied loads on the tips of the beams were monotonically raised from zero. The corresponding strains and displacements were evaluated.

Table 1
Concrete mix proportions.

Mix design	W/C	Cement kg/m^3	Water kg/m^3	Coarse aggregate kg/m^3	Fine aggregate kg/m^3
Concrete	0.35	400.0	140	990	845

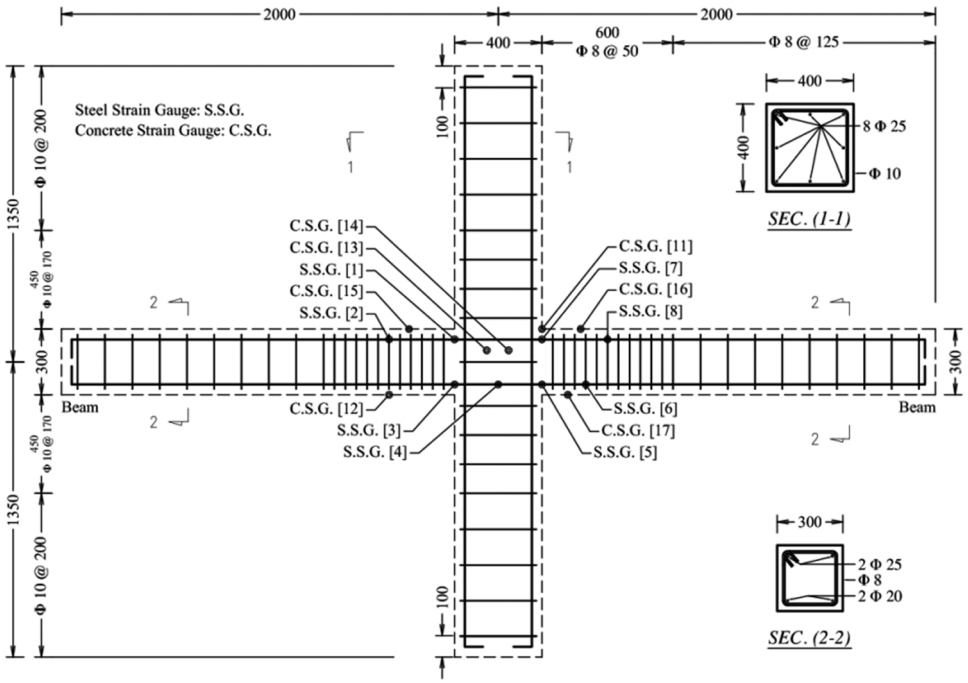

Fig. 5. Strain gauges positions and steel bars details of the control sample, J-0.

Table 2
Steel reinforcement and CFRP sheets properties.

Item	Value
Yield strength (MPa) of steel	400
Ultimate strength (MPa) of steel	560
Type of CFRP	One directional
Elastic modulus (GPa) of CFRP	240
Strain (%) of CFRP	1.05
Tensile strength (MPa) of CFRP	210
Thickness (mm) of CFRP	0.8
Density of Epoxy resin (kg/l)	1.54
Tensile strength of Epoxy resin (MPa)	13
Modulus of Elasticity of epoxy resin (GPa)	3.75

2.3. ABAQUS software

To validate and compare with the present model and experimental results, the ABAQUS software was used. The parameters used for connection in ABAQUS were listed in Table 3.

To strengthen the connections, the CFRP sheets were also fixed at special positions. To model steel bars, bar elements with behavior of elastic-perfect plastic were used. To simulate CFRP sheets, linear elastic shell elements were applied while plastic C3DBR elements were utilized to model concrete. The beam and column in the control connection were modeled by the ABAQUS software with 12,562 and 27,678 using C3D8R elements, respectively. In this study, conventional cohesive elements (COH2D4P) in the ABAQUS were employed to model the propagation of crack. A solid element with eight nodes and three translation degrees of freedom at each node are used to model the concrete. The concrete behavior was formed into a corporation in the FE model for both of the elastic and inelastic stages. In the ABAQUS software, the concrete was supposed as a homogeneous material. The compressive and tensile behavior of concrete was modeled by using the stress-strain proposed by Khalil et al. [59]. Boundary condition was simulated according to the experimental test conditions. The bottom is restrained in U1, U2, U3, UR2, UR3 and in top of the column U1, U2, UR2, UR3. It was assumed that no horizontal displacements take place at the ends of the model. Three loads are applied in step in finite element analysis that all of them were defined as pressure force: one axial load to column and two loads to the beams. Mechanical properties of materials have been extracted from the test. The interface between concrete and bars was simulated as complete bond by using the embedded technique. The assemblage reinforcement and hook and load position in the ABAQUS software are shown in Fig. 11(a) and (b), respectively.

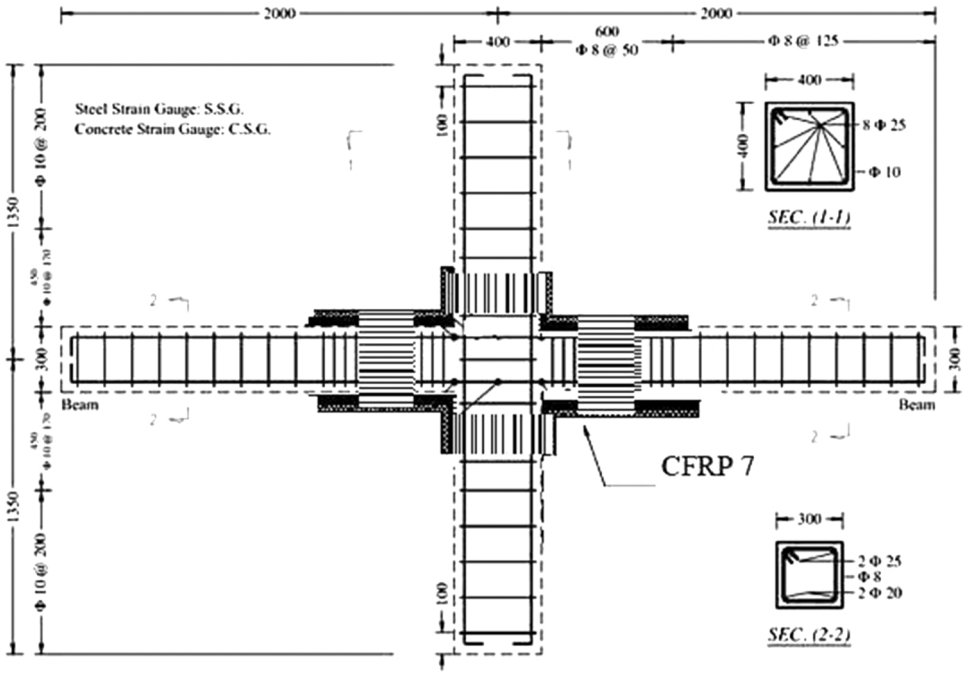

Fig. 6. Strain gauges positions and steel bars details connection strengthened with CFRP, J-1.

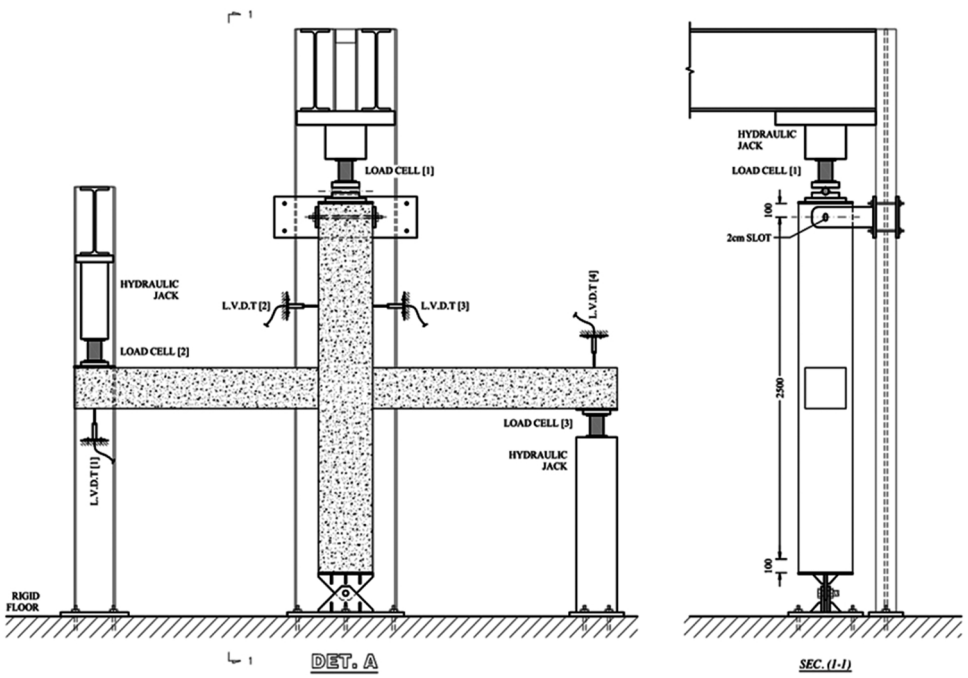

Fig. 7. Loading of sample and instrumentation.

3. Results and discussion

This part describes the comparison and validation of the propagation of crack predict by the proposed model, as well as the experimental and ABAQUS results. In the following discussion, the proposed model simulated control beam-column connection J-0 and CFRP-strengthened connection j-1 are presented.

Fig. 8. Setup of experimental test for control connection, J-0.

Fig. 9. Setup of experimental test for CFRP-strengthened connection, J-1.

Fig. 10. Supports provided for the Connection's Column.

Table 3
ABAQUS Parameters of concrete connection.

Parameters	Quantity	Explanation
$\in$	0.1	Eccentricity
ψ	56	Dilation angle (degree)
μ	0.0001	Viscosity Parameter
K	0.66	The second stress invariant/tensile meridian

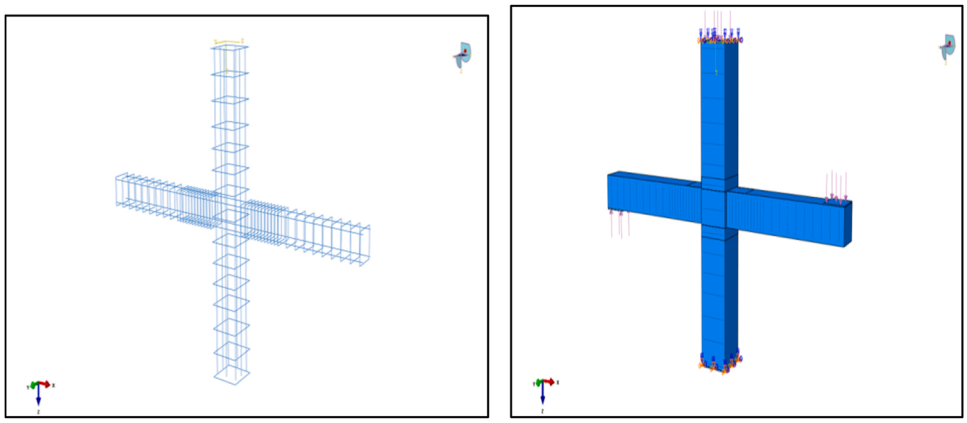

Fig. 11. Simulating of connection by ABAQUS (a) bars position and (b) Load position.

3.1. Control connection, J-0

Control connection J-0 was tested in Section 2.2.3. Fig. 12 shows the load (at the end of the beam) versus displacement diagram of control connection J-0 obtained by the proposed model, the experimental results, and the ABAQUS results. Compared with the experimental result, the load of failure in the proposed model was obtained within 7–11 % margin of difference. The load–displacement curve in the proposed model was close to that in the experimental results. On the other hand, the diagram obtained by the ABAQUS was over-predicted and presented a higher margin of difference (22–29 %) than the results of the experimental test. The failure load of the diagram in the ABAQUS (19 % difference) was unrealistic for the control connection.

Until the load reached 50 kN, the diagram presents that the it increases with linear behavior. This behavior was also reported by previous work [2,6,38]. Nonlinearity was started thereafter. In the nonlinearity part, the sample reached a maximum load equal to 318 kN at 15.1 mm displacement. The first stage of Load- deflection curve (force range of 0 up to 60 kN) exhibited linear elastic behavior for control connection (J-0). The second stage of the curve (force range about 60–130 kN) was elastic-plastic behavior due to the first cracks which happened in the top and bottom junctions of the connection. Inspection of Fig. 12 shows that steel reinforcement was yielded when 251 kN force is applied. The load- deflection curve obtained by proposed model shows a decrease in stiffness rate for control connection (J-0). It is due to concrete strength which decreases the softening and plastic deformations.

Figs. 13–15 illustrate a comparison of the cracks obtained from the proposed model and the crack patterns obtained from the experiment result as well as the findings of the ABAQUS software for the control connection (J-0). The cracks predict in the proposed model and the experiments test are similar which shows that the proposed model can simulate the crack propagation in the connection. Figs. 13 and 14 show that the first flexural crack at the beam (near to the column face) was detected in the control specimen of the proposed model and experimental test results, respectively. The beams revealed another cracks, as the load increased. At 170 kN loading, the cracks opened further about 1 mm. These discrete cracks extended to the beam depth which was reported by previous work [6,16,34]. Moreover, several small cracks created in the beam [60].

A main shear crack happened and increased with diagonal form started from the beam to the connection core. This major shear crack is not observed in the ABAQUS software as shown in Fig. 15. Compared with the eight cracks predicted in the experimental test, the proposed model obtained five cracks in the beams.

Some of the cracks may be very small to be observed in the experimental test. The control connection J-0 collapsed due to the tension steel bars yielding of the beam; based on the experimental test results. Yield point happened at about 251 kN. In the proposed model, the yield point is 267 kN and also, the curve slopes (elastic and plastic zone) are almost close to the experimental results. Also, the proposed model outcomes display that control connection J-0 collapsed due to the tension steel bars yielding. According to the proposed model, the control connection (J-0) behavior is slightly less ductile than the test results after the yield point.

The some parameters (as average values) that obtained by proposed model, experimental test, and ABAQUS are listed in Table 4. The proposed model results display suitable agreement with the observations and the findings of the experimental connection test. The

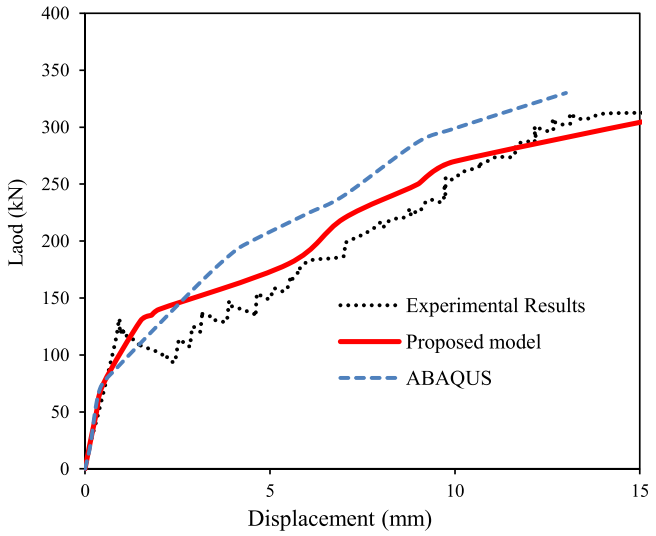

Fig. 12. Load-displacement curve for control connection, J-0.

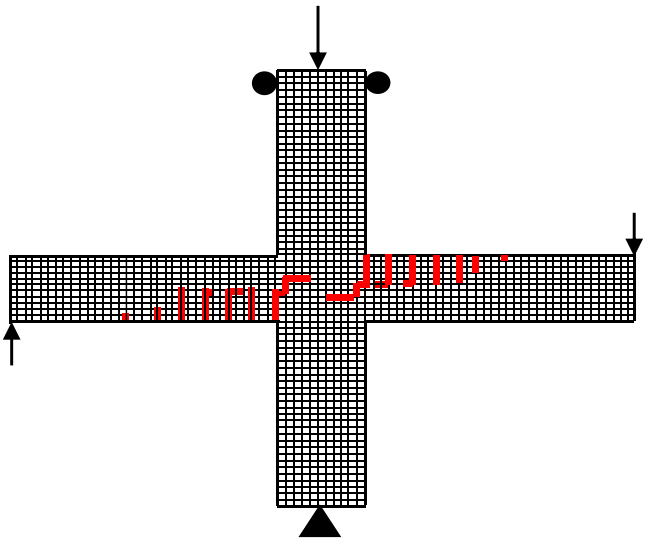

Fig. 13. Damage in the control connection simulated by the proposed model, J-0.

maximum rebar strain, moment, and displacement in the proposed model and in the experiments are close (4–9 % difference). By contrast, the results of the numerical model by the ABAQUS software were higher than that of experimental results by approximately 15.5–20.0 %.

Fig. 16 showed the longitudinal steel bar strain variations (location [7] in Fig. 5) which were obtained by the proposed model, the experimental test, and the FEM analysis using ABAQUS software. It can be seen that the results of the proposed model are close to the experimental results. Because of the catenary action, the strain was increased at the displacement of 6.6 mm in the curves obtained by the proposed model and also the experimental test results. After that, the steel bars were yielded. However, the strain in the steel bars was decreased dramatically at the end of the experimental test due to damage of strain gauge. Reviewing of Fig. 16 shows that FEM analysis result (by ABAQUS) is slightly over-estimated prediction in compared to the proposed model and the experimental test results.

3.2. CFRP strengthened join, J-1

The load–displacement result simulated by the proposed model was compared with the results of the experiment and the ABAQUS. This process is shown in Fig. 17. Fig. 17 demonstrates that the results of the experimental were close with the proposed model (8–12 % difference). The load versus displacement of the connection simulated by the ABAQUS was overpredicted compared with the present test observation (by approximately 21–28 % difference).

Fig. 14. Damage in the control connection in the experimental, J-0.

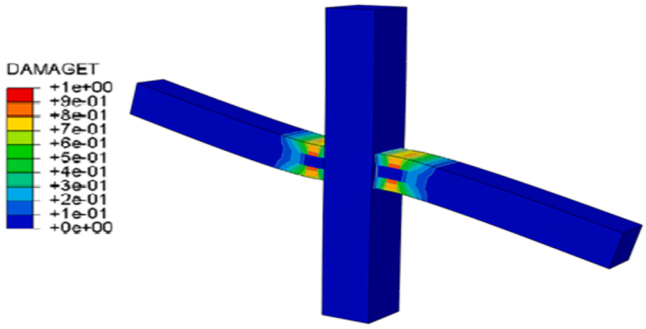

Fig. 15. Damage in the control connection simulated by BAQUS, J-0.

Table 4
Brief of experimental, proposed model and the ABAQUS results.

	Strain of the bars		Δ_{max} (mm)	M_{max} (kN m)	θ_{max} (rad)
	Column face	Beam			
Test	2.64E-03	2.64E-2	15.6	56.02	0.00621
Proposed model	2.7E-03	2.11E-2	14.9	55.26	0.00614
ABAQUS	2.8E-03	1.64E-1	11.3	54.30	0.0054

Fig. 18 shows the crack pattern in the connection strengthened by the CFRP specimen (J-1) at 300 kN. Fig. 19 shows a crack pattern in the experimental test. Fig. 20 illustrates the crack pattern by the ABAQUS. The predicted cracking in the experimental observations is consistent with the proposed mod results. By using the CFRP sheets, no crack was detected on the surface of the column or on connection core. The cracks length reduced due to the application of CFRP sheets. The average reduction is about 37 % of the length of crack compared with the control connection. The crack form found by the ABAQUS were predicted only one crack in the beams. The load- deflection curve of connection with CFRP is showed elastic behavior at initial stages of loading (up to 110 kN). However, at the second stages (force range of 110–200 kN), the curve was changed to the elastic-plastic behavior since the first cracks happened in the beam. The load- deflection curve showed a decrease in stiffness due to concrete strength which decrease softening and plastic deformations. In the beam, Figs. 18 and 19 illustrate that a flexural crack initially appear near the CFRP sheets. Also, two cracks were remarked in the top half of both beams about 200 mm lenght due to the presence o CFRP sheets. Small crack was detected about 50 mm lenght. The flexural cracks began to grow upward in the beam, as the load increased. Flexural cracks extended into the lower half of the beam. The main cracks close to the CFRP propagated to approximately 3/4th of the beam depth when the load was approximately 300 kN. The failure mechanism before retrofit was the connection shear. It was observed at failure load that debonding happened between boundaries of the CFRP and concrete for the strengthened beam-column connection. This CFRP sheets stopped the propagation of cracks in the connection. Strengthening shifted failure to the beam.

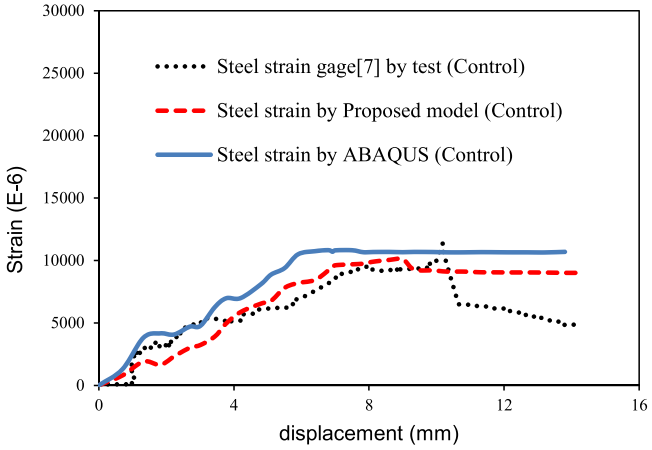

Fig. 16. Variation of longitudinal bar strain of control joint (J-0).

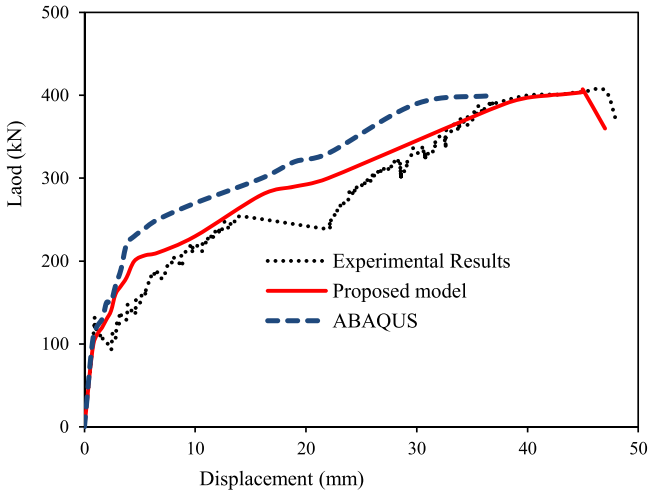

Fig. 17. Load versus displacement curve of connection CFRP-strengthened, J-1.

The strengthened connection by CFRP can considerably increase the displacement and ultimate load as shown in Fig. 21. The connection strengthened by CFRP showed strength and displacement of approximately 78 % and 98 %, respectively. Based on the results obtained by the proposed model, the connection strengthened with CFRP performed better than the control beam in terms of displacement. The average decrease in the length of the crack in the control connection was approximately 37 %. For the strengthened connection, cracks happened at a comparatively higher load than, compare to the control connection, based on the results obtained by the proposed model. The failure mode observed on the beam—column connection strengthened by CFRP significantly improved crack prevention. The CFRP sheets stopped cracks propagating and preserved the original shape of connection. The results obtained by the proposed model confirm that strengthening can manage propagations and decrease the length of cracks. The results of the experimental test verify these findings that was also reported by previous works [46,48].

3.3. Parametric study

To show the effect of different parameters such as number of CFRP layers, column axial load and concrete comprehensive strength, the parametric study has been conducted on the proposed model. Fig. 22(a) shows that the ultimate load, initial stiffness, and also energy absorption (The area of Curves) increased with increase of number of CFRP layers as reported by other published researchers [10,26]. The load–displacement curves of CFRP strengthened joint with different column axial load are shown in Fig. 22(b) which reveals the effectiveness of column axial load on enhancing the CFRP strengthened joint behavior by increase of its ultimate load, initial stiffness, post cracking stiffness, and energy dissipation. The similar findings were also reported by other published researchers [3,5,13].

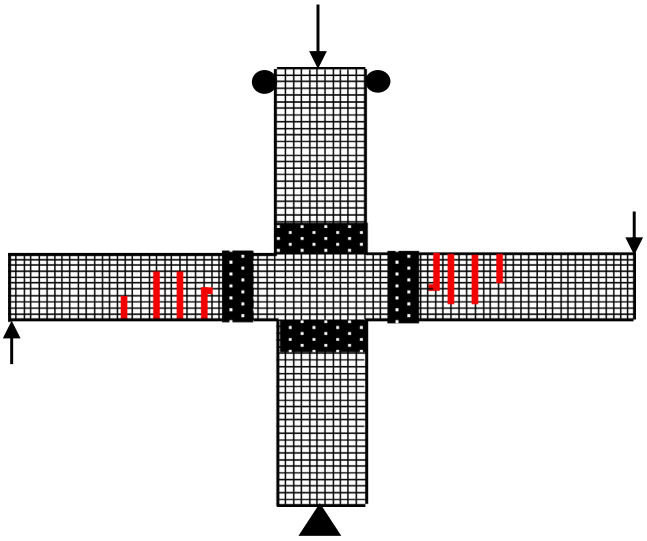

Fig. 18. Damage of strengthened connection simulated by the proposed Model, J-1.

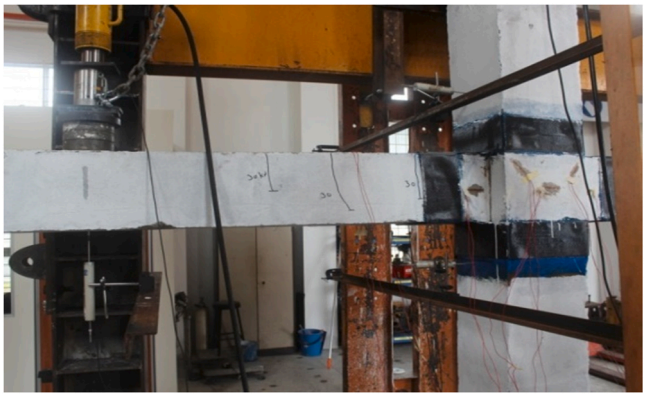

Fig. 19. Damage of the connection in experimental test, J-1.

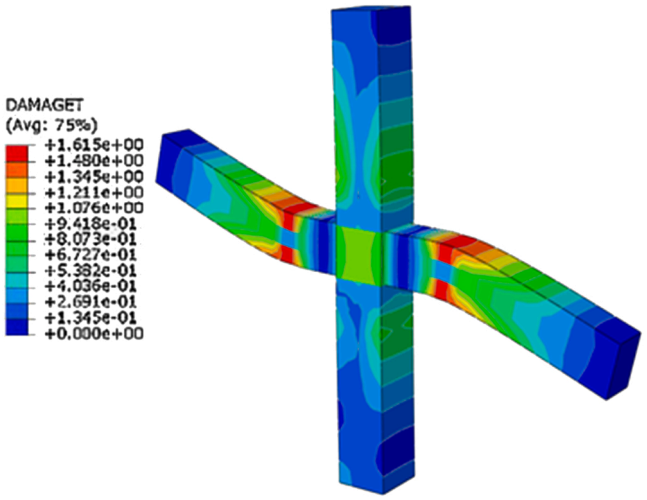

Fig. 20. Damage for connection simulated by ABAQUS, J-1.

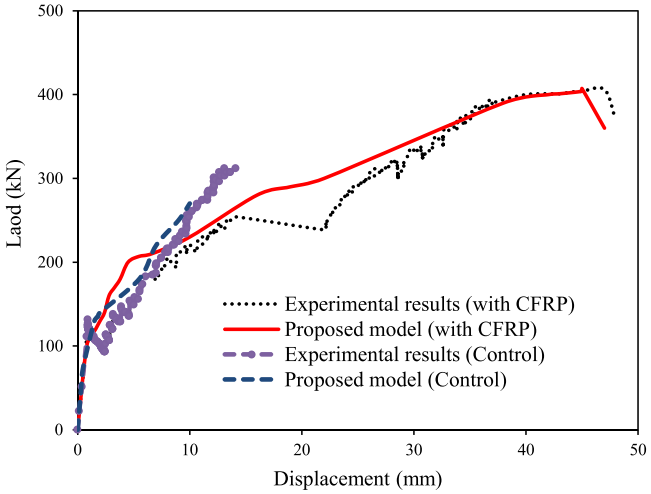

Fig. 21. Comparisons of load versus displacement curves.

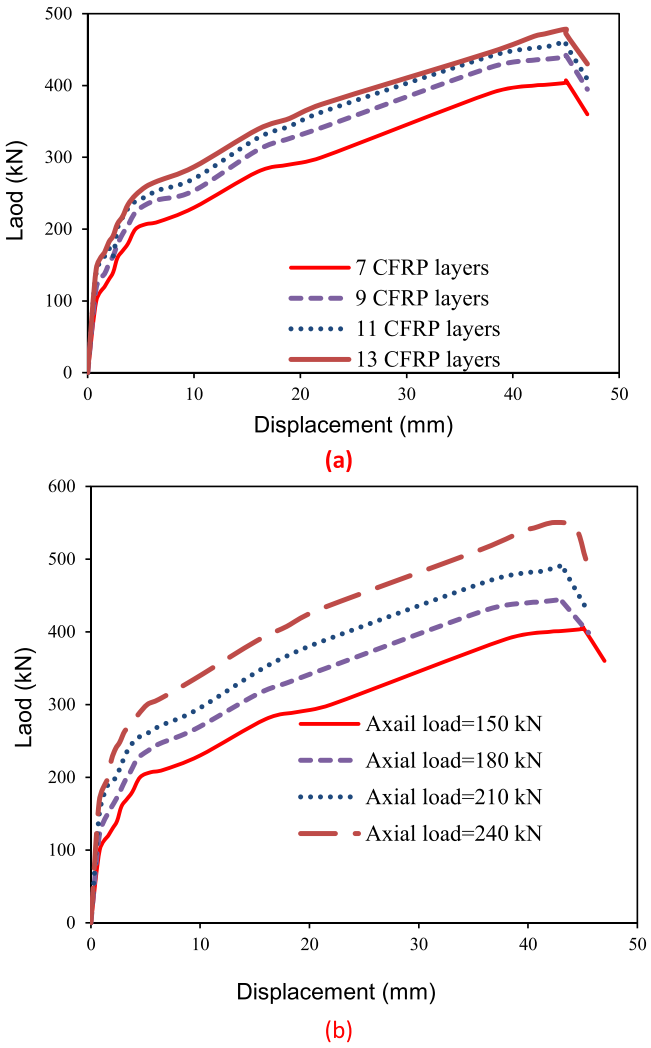

Fig. 22. Load–displacement curves with different (a) number of CFRP layers and (b) column axial load.

4. Conclusions

A finite element model was developed to simulate propagation of the crack in the beam-column connection. In order to validate the proposed model, experimental tests were conducted on an RC connection as the control connection and on a CFRP-strengthened connection. The conclusions can be described as below.

- The crack directions at the tensile area in the experimental tests and the proposed model were close to each other. In the proposed model and in the experimental results, initially, cracks of flexural at the bottom of the beam adjacent to the column face were detected in the control specimen.
- The results shows that the ultimate load, initial Stiffness, and also energy absorption increased with increased number of CFRP layers.
- Load–displacement curves of CFRP strengthened joint with different column axial load reveals that the effectiveness of column axial load for enhancing the CFRP strengthened joint behavior by increasing its ultimate load, initial stiffness, post cracking stiffness, and energy dissipation.
- Additionally, the proposed model was improved to simulate propagation of the crack in strengthened connections. The proposed model results demonstrated excellent harmony with the experimental observations (approximately 8–12 % difference), whereas the ABAQS software results were considerably greater than that of the experimental results (approximately 21–28 %).
- It was also observed in the beam that propagation of the crack was managed by the CFRP sheets. The crack length of the control beam column connection was decreased by approximately 37 %. The failure mechanism before retrofitting was in connection shear.
- Using CFRP stopped the propagation of the cracks in the connection and shifted failure to the beam area.

Declaration of Competing Interest

The authors declare that they have no known competing financial interests or personal relationships that could have appeared to influence the work reported in this paper.

Data Availability

Data will be made available on request.

Acknowledgements

The authors gratefully acknowledge the contribution of the Slovak Research and Development Agency under the project APVV-20-0261. In addition, this research is partially supported by the European Union's Horizon 2020 Research and Innovation Programme under the Programme SASPRO 2 COFUND Marie Sklodowska-Curie under Grant 945478.

References

[1] J.B. Deaton, Nonlinear Finite Element Analysis Of Reinforced Concrete Exterior Beam-column Joints With Nonseismic Detailing (Thesis), School of Civil and Environmental Engineering Georgia Institute of Technology, 2013.
[2] Y.B.A. Tahnat, M.A. Samaaneh, M.M.S. Dwaikat, Simple equations for predicting the rotational ductility of fiber-reinforced-polymer strengthene dreinforced concrete joints, Structures 24 (2020) 73–86.
[3] F. Gao, Z. Tang, S. Mei, B. Hu, S. Huang, J. Chen, Seismic behavior of exterior beam–column joints with experimental and numerical investigations, Adv. Struct. Eng. 24 (1) (2021) 90–106.
[4] B. Abdelwahed, S, M.R. Kaloop, W.E. El-Demerdash, Nonlinear numerical assessment of exterior beam-column connections with low-strength concrete, Buildings 11 (11) (2021) 562.
[5] R.Z. Al-Rousan, Cyclic behavior of alkali-silica reaction-damaged reinforced concrete beam-column joints strengthened with FRP composites, Case Stud. Constr. Mater. 16 (2022), e00869.
[6] R. Chitra, S.J. Mohan, Reinforced concrete beam-column joint's ductility behavior, Mater. Today: Proc. 51 (1) (2022) 1069–1073.
[7] R. Al-Rousan, Behavior of B-C connections damaged by thermal shock, Mag. Civ. Eng. 99 (2020) 7.
[8] J. Tryding, M. Ristinmaa, Normalization of cohesive laws for quasi-brittle materials, Eng. Fract. Mech. (2022) (In Press).
[9] G. Liu, D. Zhou, Y. Bao, J. Ma, Z. Han, Multiscale simulation of major crack/minor cracks interplay with the corrected XFEM, Arch. Civ. Mech. Eng. 2 (2017) 410–418.
[10] R. Al-Rousan, O. Nusier, K. Abdalla, M. Alhassan, N.D. Lagaros, NLFEA of sulfate-damaged circular CFT steel columns confined with CFRP composites and subjected to axial and cyclic lateral loads, Buildings 12 (3) (2022), 12030296, 296.
[11] A.M. Said, M.L. Nehdi, Use of FRP for RC frames in seismic zones: Part I. Evaluation of FRP beam-column joint rehabilitation techniques, Appl. Compos. Mater. 11 (2004) 205–226.
[12] M.A. Alhassan, R.Z. Al-Rousan, L.K. Amaireh, M.H. Barfed, Nonlinear finite element analysis of B-C connections: influence of the column axial load, jacket thickness, and fiber dosage, Structures 16 (2018) 50–62.
[13] F. Gao, Z. Tang, B. Hub, J. Chen, H. Zhu, J. MA, Investigation of the interior RC beam-column joints under monotonic antisymmetrical load, Front. Struct. Civ. Eng. 13 (2019) 1474–1494.
[14] A. Parvin, S. Wu, Ply angle effect on fiber composite wrapped reinforced concrete beam-column connections under combined-axial and cyclic loads, Compos. Struct. 82 (4) (2008) 532–538.
[15] T. Skuturna, J. Valivonis, The statistical evaluation of design methods of the load-carrying capacity of flexural reinforced concrete elements strengthened with FRP, Arch. Civ. Mech. Eng. 15 (1) (2015) 214–222.

[16] M. Abdallah, F.A. Mahmoud, M.I. Tabet-Derraz, A. Khelil, J. Mercier, Experimental and numerical investigation on the effectiveness of NSM and side-NSM CFRP bars for strengthening continuous two-span RC beams, J. Build. Eng. 41 (2021), 102723.
[17] A. Ebanesar, H. Gladston, E.N. Farsangib, S.V. Sharma, Strengthening of RC beam-column joints using steel plate with shear connectors: experimental investigation, Structures (2021).
[18] C.P. Pantelides, Y. Okahashi, D. Reaveley, Seismic rehabilitation of reinforced concrete frame interior beam-column joints with FRP composites, J. Compos. Constr. (2008) 435–445.
[19] T. Supaviriyakit, A. Pimanmas, P. Warnitchai, Nonlinear finite element analysis of non-seismically detailed interior reinforced concrete beam-column connection under reversed cyclic load, ScienceAsia 34 (2008) 049–058.
[20] K.R. Bindhu, K.P. Jaya, Strength and behaviour of exterior beam column joints with diagonal cross bracing bars, Asian J. Civ. Eng. 11 (3) (2010) 397–410.
[21] H. Zhou, Z. Zhang, Interaction of internal forces of exterior beam-column joints of reinforced concrete frames under seismic action, Struct. Eng. Mech. 44 (2) (2012) 197–217.
[22] S. Prabavathy, S. Rajagopal, Study of exterior beam-column joint with different joint core and anchorage details under reversal loading, Struct. Eng. Mech. 46 (6) (2013) 809–825.
[23] A. Masi, G. Santarsiero, A. Mossucca, Influence of axial load on the seismic behavior of RC beam-column joints with wide beam, Appl. Mech. Mater. 508 (2014) 208–214.
[24] I. Fadwa, T.A. Ali, E. Nazih, M. Sara, Reinforced concrete wide and conventional beam–column connections subjected to lateral load, Eng. Struct. (2014) 34–48.
[25] S.M. Kulkarni, Y. Patil, A novel reinforcement pattern for exterior reinforced concrete beam column joint, Procedia Eng. 51 (2014) 184–193.
[26] K.M. Abdalla, R. Al-Rousan, M.A. Alhassan, N.D. Lagaros, Finite-element modelling of concrete-filled steel tube columns wrapped with CFRP, Struct. Build. 173 (11) (2020) 844–857.
[27] A.K. Kaliluthin, S. Kothandaraman, T.S. Aha, A review on behavior of reinforced concrete beam column joint, Int. J. Innov. Res. Sci. Eng. Technol. 3 (4) (2014) 11299–11312.
[28] R. Kiran, G. Genesio, A case study on pre 1970s constructed concrete exterior beam-column joints, Case Stud. Struct. Eng. (2014) 20–25.
[29] S. Rajagopal, S. Prabhavaty, Behaviour of exterior beam column joint using mechanical anchorage under reversal loading: an experimental study, IJST Trans. Civ. Eng. 38 (2) (2014) 345–358.
[30] G. Fan, Y. Song, L. Wang, Experimental study on the seismic behavior of reinforced concrete beam-column joints under various strain rates, J. Reinf. Plast. Compos. (2014) 601–618.
[31] R.Z. Al-Rousana, M.A. Alhassan, R.J. Al-omary, Response of interior beam-column connections integrated with various schemes of CFRP composites, Case Stud. Constr. Mater. 14 (2021), e00488.
[32] R.S. Patel, B. Nambiyanna, R. Prabhakara, An experimental study on effect of diameter of rebar on exterior beam column joint, Int. J. Innov. Res. Sci. (2015) 5984–5991.
[33] C. Del Vecchio, M. Di Ludovico, A. Balsamo, A. Prota, G. Manfredi, M. Dolce, Experimental investigation of exterior RC beam-column joints retrofitted with FRP systems, J. Compos. Constr. 18 (4) (2022) (In Press).
[34] V. Rodríguez, H. Guerrero, S.M. Alcocer, E. Tapia-Hernández, Rehabilitation of heavily damaged beam-column connections with CFRP wrapping and SFRM casing, Soil Dyn. Earthq. Eng. 145 (2021), 106721.
[35] M. Moskaleva, A. Safonov, E. Hernández-Montes, Fiber-reinforced polymers in freeform structures: a review, Buildings 11 (10) (2021) 481.
[36] R.Z. Al-Rousan, A. Alkhawaldeh, Behavior of heated damaged reinforced concrete beam-column joints strengthened with FRP, Case Stud. Constr. Mater. 15 (2021), e00584.
[37] K. Sakthimurugan, K. Baskar, Experimental investigation on rcc external beam-column joints retrofitted with basalt textile fabric under static loading, Compos. Struct. 268 (2021), 114001.
[38] M. Deng, M. Zhang, Z. Zhu, F. Ma, Deformation capacity of over-reinforced concrete beams strengthened with highly ductile fiber-reinforced concrete, Structures 29 (2021) 1861–1873.
[39] R.Z. Al-Rousan, A. Alkhawaldeh, Numerical simulation of the influence of bond strength degradation on the behavior of reinforced concrete beam-column joints externally strengthened with FRP sheets, Case Stud. Constr. Mater. 15 (2021), e00567.
[40] A. Parvin, S. Altay, C. Yalcin, O. Kaya, CFRP rehabilitation of concrete frame joints with inadequate shear and anchorage details, J. Compos. Constr. 14 (1) (2010) 72–82.
[41] M. Ludovico, G.P. Lignola, A. Prota, E. Cosenza, Nonlinear analysis of cross sections under axial load and biaxial bending, ACI Struct. J. 107 (4) (2010) 390–399.
[42] U. Akguzel, S. Pampanin, Effects of variation of axial load and bidirectional loading on seismic performance of GFRP retrofitted reinforced concrete exterior beam-column joints, J. Compos. Constr. 14 (1) (2011) 94–104.
[43] U. Akguzel, S. Pampanin, Assessment and design procedure for the seismic retrofit of reinforced concrete beam-column joints using FRP composite materials, J. Compos. Constr. 16 (1) (2012) 21–34.
[44] M. Alhaddad, N. Siddiqui, A. Abadel, S. Alsayed, Y. Al-Salloum, Numerical investigations on the seismic behavior of FRP and TRM upgraded RC exterior beam-column joints, ASCE, J. Compos. Constr. 16 (3) (2012) 308–321.
[45] S. Xiaobing, G. Xianglin, L. Yupeng, T. Chang, Z. Weiping, Mechanical behavior of FRP-strengthened concrete columns subjected to concentric and eccentric compression loading, J. Compos. Constr. (2013) 36–346.
[46] V. Singh, P.P. Bansal, M. Kumar, S.K. Kaushik, Experimental studies on strength and ductility of CFRP jacketed reinforced concrete beam-column joints, Constr. Build. Mater. 55 (2013) 194–201.
[47] R. Realfonzo, A. Napoli, J.G.R. Pinilla, behavior of RC beam-column joints strengthened with FRP systems, Constr. Build. Mater. 54 (2014) 282–297.
[48] K. Bsisu, B.O. Hiari, Finite element analysis of retrofitting techniques for reinforced concrete beam-column joint, J. Am. Sci. 11 (8) (2015) 48–56.
[49] H. Baji, A. Eslami, H.R. Ronagh, Development of a nonlinear FE modelling approach for FRP-strengthened RC beam-column connections, Structures (2015) 272–285.
[50] L.R. Taylor, FEAPpv Source, A Finite Element Analysis Program, Personal Version, University of California, Berkeley, 2009.
[51] Y. Goto, O. Joh, An experimental study on shear failure mechanism of RC interior beam-column joint, in: Proceedings of the Eleventh World Conference on Earthquake Engineering, Acapulco, México, 1996.
[52] N. Mitra, L.N. Lowes, Evaluation, calibration, and verification of a reinforced concrete beam–column joint model, J. Struct. Eng. 133 (1) (2007) 105–120.
[53] D. Xie, A.G. Salvi, C. Sun, A.M. Waas, A.I. Caliskan, Discrete cohesive zone model to simulate static fracture in 2D triaxially braided carbon fiber composites, J. Compos. Mater. 40 (22) (2006) 2025–2046.
[54] S. Shahbazpanahi, M. Paknahad, Simulation of the mode I fracture of concrete beam with cohesive models, J. Comput. Appl. Mech. 48 (2) (2017) 207–216.
[55] D. Xie, A.M. Waas, Discrete cohesive zone model for mixed-mode fracture using finite element analysis, Eng. Fract. Mech. 73 (13) (2006) 1783–1796.
[56] S. Shahbazpanahi, A. Kamgar, Fracture modelling of crack propagation in steel, in: ICCEN 2013: December 13–14, Stockholm, Sweden, 2014, pp. 197–201.
[57] S. Shahbazpanahi, A. Kamgar, A novel numerical model of debonding of FRP-plated concrete beam, J. Chin. Inst. Eng. 38 (1) (2014) 24–32.
[58] ASTM C39/C39M, Standard Test Method for Compressive Strength of Cylindrical Concrete Specimens, 2014.
[59] A.E.H. Khalil, E. Etman, A. Atta, M. Essam, Nonlinear behavior of RC beams strengthened with train hardening cementitious composites subjected to monotonic and cyclic loads, Alex. Eng. J. 55 (2016) 1483–1496.
[60] S. Marimuthu, G.S. Pillai, Experimental investigation of exterior reinforced concrete beam-column joints strengthened with hybrid FRP laminates, Građevinar 4 (2021) 365–379.